

Latitudinal Dependence of Ionospheric Responses to Some Geomagnetic Storms during Low Solar Activity

B. W. Joshua^{a, *}, J. O. Adeniyi^b, A. O. Olawepo^c, Babatunde Rabi^{d,f}, Okoh Daniel^{d,f}, S. J. Adebisi^b, B. O. Adebisin^b, S. O. Ikubanni^b, and B. Abdurahim^e

^a Department of Physics, Kebbi State University of Science and Technology, Aliero, Kebbi State, Nigeria

^b Department of Physics, Landmark University, Omu-Aran, Kwara State, Nigeria

^c Department of Physics, University of Ilorin, Ilorin, Kwara State, Nigeria

^d Center for Atmospheric Research, National Space Research and Development Agency, Anyigba, Nigeria

^e National Space Research and Development Agency (NASRDA) Abuja, Nigeria

^f Institute for Space Science and Engineering, African University of Science and Technology, Abuja, Nigeria

*e-mail: benjaminjoshua7@gmail.com

Received July 2, 2020; revised September 17, 2020; accepted January 28, 2021

Abstract—The Latitudinal dependence in the response of the Ionospheric F_2 -layer electron density (NmF_2) and peak height (hmF_2) to three geomagnetic storms of May and August 2010 has been examined. The data-sets used for the study were obtained from Ilorin, Nigeria (1.87° S/ 76.67° E), San Vito, Italy (34.68° N/ 90.38° E), Hermanus, South Africa (42.34° S/ 82.15° E), and Pruhonice, Czech Republic (45.66° N/ 90.38° E) geomagnetic coordinates. The quiet time result shows that the rise in NmF_2 began earlier at San Vito, followed by Pruhonice. The rate of ionization was observed to be highest in Ilorin, while, the rate of decay in NmF_2 is faster at Hermanus. For disturbed NmF_2 condition, remarkable similarities in the NmF_2 responses during geomagnetic storms were recorded from Hermanus in the mid-latitude and Ilorin, an equatorial station. NmF_2 enhancements (>6 hours) that is consistent with the increase in hmF_2 were observed at all the mid-latitude stations during the main phase of the 02 May, 2010 storm, without any noticeable change over ILN. Similarly, 12 hours of positive phase was observed at ILN and HMN, with 30 hours of NmF_2 depletions at PRN and SVT during the recovery phase. ILN is in the equatorial Trough, so most of the NmF_2 produced at this region is lifted to the higher latitudes by the fountain effect during the main phase. The suppression of the zonal electric field at ILN is responsible for the NmF_2 enhancement during the recovery phase, while the mid-latitude responses have been attributed to the effect of the thermospheric winds and neutral composition changes.

Keywords: electron density, peak height, geomagnetic storms, electric field, magnetosphere

DOI: 10.1134/S0016793221030063

1. INTRODUCTION

The earth's ionosphere is the region of the upper atmosphere that is ionized by solar radiation, thus having sufficient amount of electrons that can influence radio propagation. Geomagnetic storms usually have effects on the distribution of ionospheric electron densities, leading to the phenomenon otherwise referred to as Ionospheric storm which in turn can lead to adverse effects on ground and space based communication and navigation systems (Titheridge and Buonsanto, 1988).

Geomagnetic storms generally occur once there is a rapid change in the magnetic field caused by coronal mass ejections (CMEs) aimed at the Earth from the sun (Reeves, 2010). This can cause an increase in the ram pressure characterized by unexpected increase in the speed, temperature and density of the solar wind as

well as changes in the orientation of the interplanetary magnetic field (IMF) B_z (Shweta et al., 2012).

It has been shown by Tsurutani et al., (1990) and Gonzalez et al. (1994) that the IMF B_z is the main parameter that determines the occurrence of geomagnetic storms. This is because the release of energy into the magnetosphere is directly dependent on the magnitude and direction of the IMF B_z (Shweta et al., 2010), particularly when it is southward. This usually leads to inter-connections with Earth's magnetic field, and consequently the flow of CME into the earth's magnetosphere. When these CMEs hit the Earth's magnetosphere, disturbances in the ionosphere usually follow.

Kamide et al. (1998) identified four mechanisms that are the primary causes of the increase in solar wind electric field that is responsible for the formation of geomagnetic storms. The mechanisms include:

interplanetary corona mass ejections (ICMEs or just CME), co-rotating interaction regions (CIRs), Alfvénic IMF fluctuations, and the Russel-Mcpherron effect. He further explained that, ICMEs and CIRs are the leading events (major drivers) in the formation of geomagnetic storms, while Alfvénic IMF fluctuations and the Russel-Mcpherron effect are modifiers; they don't have the capacity of causing geomagnetic storms without any CME or CIR. CMEs are more frequent near the solar maximum; they are responsible for most geomagnetic storms that occur during the high solar activity as well as other stages or phases of the solar cycle (Gostling et al., 1991; Webb and Howard, 1994; Taylor et al., 1994; Kamide et al., 1998). Strong CIRs are said to occur mostly during the decreasing or descending stage of the solar cycle (Kamide et al., 1998; Tsurutani et al., 1995).

The Disturbance Storm Time (*Dst*) index is the parameter used to describe the strength of a geomagnetic storm (Gonzalez et al., 1994; Kamide et al., 1998). It is a measure of the decrease in the Horizontal (*H*) component of the Earth's magnetic field. This decrease in the *H*-field is usually caused by the increase in the ring current that surrounds the earth during geomagnetic storms. The most significant characteristic of any geomagnetic storm is the intensification of the ring current and its consequent recovery (Gonzalez et al., 1994 and Kamide et al., 1998, Bousanto, 1999), thus leading to the various phases of the geomagnetic storm. A typical geomagnetic storm has three most important phases; the initial phase (usually characterized by a sudden rise in the *H*-field (*Dst* index) known as Sudden Storm Commencement (SSC)), main phase (a gradual negative growth in the *Dst* index) and the recovery phase (a gradual rise in *Dst* from its minimum negative value), although, not all geomagnetic storms start with an SSC (Gonzalez et al., 1994 and Kamide, 1998). Apart from the *Dst* index, other geomagnetic indices like; Aurora Electrojet (AE), strength of the symmetric ring current (SYM-H), the planetary indices (*Kp* and *Ap*) are also used in describing a geomagnetic storm event.

Geomagnetic storm effects are known to be characterized by both *NmF2* enhancements and depletions otherwise known as the positive and negative phase respectively. However, *NmF2* responses vary significantly (even on quiet days); from one latitudinal region to the other, with seasons of the year, local time, as well as the intensity or nature of the geomagnetic disturbance (Essex et al., 1981; Adeniyi, 1986; Titheridge and Buonsanto 1988; Buonsanto, 1999; Mansilla, 2004; Kumar et al., 2005, etc.). Changes in the equatorial zonal electric field, chemical composition and neutral wind have been reported during geomagnetic storm events (Fejer, 1998; Sastri et al., 2000) and are known to also influence the *NmF2* responses during such periods. Earlier studies such as Martyn (1947), Skinner and Wright, (1955), Rastogi et al., (1972); have attributed the movement of ionization in

the equatorial and the low latitude to the cross field of the electric and the magnetic fields otherwise known as the ExB force.

Previous and recent studies (Skinner and Wright, 1955, Low and Roelofs, 1973, Woodman, 1970, Turunen and Rao, 1980, Adeniyi, 1986, Radicella and Adeniyi, 1999, Burns et al., 2007, Adebesein, 2008, Joshua et al., 2011, Adewale et al., 2011, Olawepo et al., 2012, Adebisi et al., 2012, Adekoya et al., 2012, Akala et al., 2013, Joshua et al., 2013, Herberulema, 2013, Joshua et al., 2014a, 2014b, Adebisi et al., 2014, Joshua et al., 2018) have reported positive storm effect as prominent *NmF2* and Total Electron Content (TEC) responses of the equatorial/low latitude region and negative storms to be dominant at the mid and high latitudes.

Two physical processes are known to be responsible for some of the complex variations of the zonal electric fields and plasma drifts in the equatorial *F*-region during geomagnetically disturbed conditions. These processes include: the Prompt Penetration Electric Field (PPEF) and the Disturbance Dynamo Electric Fields (DDEF). Kelley et al., (1979) had earlier attributed the generation of the PPEF to the rotation of the interplanetary magnetic field (IMF *Bz*) either southwards or northwards. The PPEF has been linked with the solar wind and the magnetosphere dynamo (Senior and Blank, 1984) and its effects cover a range of latitudes from mid-latitudes to equatorial and low latitudes occurring at the same time (Shweta et al., 2012). The ionospheric DDEF proposed by Blank and Richmond (1980), are said to be generated by the changes in the global circulation induced by Joule heating at aurora latitudes during geomagnetic storms (Blanc and Richmond, 1980; Sastri, 1988; Scherliess and Fejer, 1997).

The peculiarity of the equatorial and low latitude ionosphere and its response to space weather events has been a matter of intense research across the globe (Manju et al., 2009). Interestingly, part of Africa falls within the equatorial latitude. However, the paucity of ionospheric observatories in the African sector accounts for the insufficient number of studies on the ionospheric *F2*-layer responses to geomagnetic storms reported in literatures from the region. Therefore, the need for more studies on geomagnetic storms and related events cannot be overemphasized, for a better modeling of the storm time ionosphere, especially in the African sector. This study presents the latitudinal dependence of the response of the ionospheric *F2*-layer peak parameters to the moderate geomagnetic storms that occurred in the months of May and August, 2010; a year of extreme solar minimum ($F10.7 = 81$ solar flux unit and sunspot number 16.5). These geomagnetic storms fall among the moderate geomagnetic storms that were recorded during the period of low solar activity since 2008.

There is however a number of studies from different sectors on the geomagnetic storm events that occurred particularly in 2010 using different approaches and

techniques. For instance; Valladares et al. (2017) studied the magnetic storms of 3–4 August 2010 and 5–6 August 2011, using the Ground- and space-based observations over the low-, mid- and high latitudes of the American continent. Their results reveal an early equatorial anomaly that has no poleward expansion beyond 20° geomagnetic latitude. They also reported two significant enhancements in TEC at the Mid-latitude, showing a complex pattern of structure and mapping, which is independent of the equatorial and low latitude fountain effect. Sheng et al. (2017) investigated the thermospheric temperature and density recovery during the April 5, 2010 geomagnetic storms and were able to test the sensitivity of thermospheric temperature and density recovery rates to nitric oxide cooling after geomagnetic storms. Baishev et al. (2015) studied the magnetic and ionospheric disturbances at Paratunka, Yakutsk as well as in the far eastern region of Russia during 5th April, 2010 geomagnetic storm. They estimated the wavelet powers of geomagnetic perturbations at different stations performing wavelet analysis of the experimental data. Their results reveal the presence of weak geomagnetic disturbances that precedes the main phase of the storm. They further reported the presence of the F_2 layer electron density pre-storm enhancement on the 4th April, 2010 as also a prolonged negative storm effect during the main and recovery phase of the geomagnetic storm. Smimov (2014) on the other hand reported a decrease in air conductivity four (4) hours before the storm, and lasted for twenty (20) hours, in his study of the reaction of electric and meteorological states of the near-ground atmosphere during April 5, geomagnetic storm. Adebisi et al. (2014) investigated the F_2 layer response to the geomagnetic storm events of 5–7 April 2010, using data from two stations each from the low- and mid- latitude stations, although at different longitudes. Their findings reveal simultaneous NmF_2 enhancements at the equatorial station and NmF_2 depletions at the mid-latitude. Shiemes et al., 2012 investigated the signature of the coronal hole near the north crest equatorial anomaly over Helwan and Aswan in Egypt, using multi-instruments (GPS and MAGDAS) during the April 5, geomagnetic storm. Their result shows the occurrence of both positive and negative storm effect as well as a strong night time enhancement. They associated the negative storm effect to the daytime ionospheric dynamo as a result of the long period of corona hole and southward orientation of the IMF B_z during the recovery period of the storm. They also reported the occurrence of the pre-reversal phenomena otherwise known as the night time enhancement during this geomagnetic storm.

It is evident that there are more studies on the April 5, 2010 geomagnetic storm than the other storms of the same year reported in literature. This may not be unconnected with the fact that it was the first geomagnetic storm in the epoch of low solar activity in 2010. Also, most of these studies focused on a particular

region or sector. Ionospheric responses to geomagnetic storms have been broadly studied for several decades, but there are still features that are yet to be completely understood (Astafyeva et al., 2015). The current study therefore is aimed at investigating and providing more insight into the variations in NmF_2 with respect to latitude during the geomagnetic storms of May and August, 2010. The NmF_2 response from a station in the equatorial trough in the African sector was investigated, alongside three other stations in the mid-latitude. These stations were selected along a close range of longitude but at different latitude, to minimize the local time effect. For a better analysis of the storm time NmF_2 , we have in this study considered the variation of the quiet time F_2 -layer ionospheric profiles for these stations as a reference condition for the geomagnetic storm analysis.

2. DATA AND METHOD

The hourly values of the ionospheric peak parameters (i.e. foF_2 and hmF_2) used for this study for Ilorin were obtained from the Archive of the DPS 4 Digisonde, installed at the University of Ilorin ionospheric Observatory which is in a Standard Archiving Output (SAO) format. The foF_2 and hmF_2 for the other stations were obtained from the National Geophysical Data Center (NGDC) <http://spidr.ngdc.noaa.gov/spidr/dataset.do> and has been saved in our archive. However, this sight has been shut down for many years now, but the same data can be obtained from the website of the University of Massachusetts Lowell center for atmospheric research (<http://ulcar.uml.edu/stationlist.html>).

The corresponding NmF_2 values were estimated from foF_2 values for all hours, using the usual relationship in equation 1;

$$NmF_2 = \frac{(foF_2)^2}{80.5}. \quad (1)$$

The geographic locations of the stations used in this study are shown in Fig. 1, while the lists of the Digisonde/ionosonde stations as well as their coordinates are shown in Table 1.

The interplanetary parameters used consist of the hourly values of the interplanetary magnetic field (IMF B_z) and the interplanetary electric field (IEF E_y); the solar wind speed (V_x); while the geomagnetic storm indices used are the disturbance storm time (Dst) index, the planetary K index (Kp), the aurora electrojet indices such as; AE and AL indices. These parameters were obtained from National Space Science Data Center (NSSDC), OMNI database (<http://nssdc.gsfc.nasa.gov/omniweb>). The Images of the O/N_2 ration global maps for 30 April to 05 May, 2010 obtained from the Global Ultraviolet Imager (GUVI) website: <http://guvitimed.jhuapl.edu/guvi-galleryl3on2>.

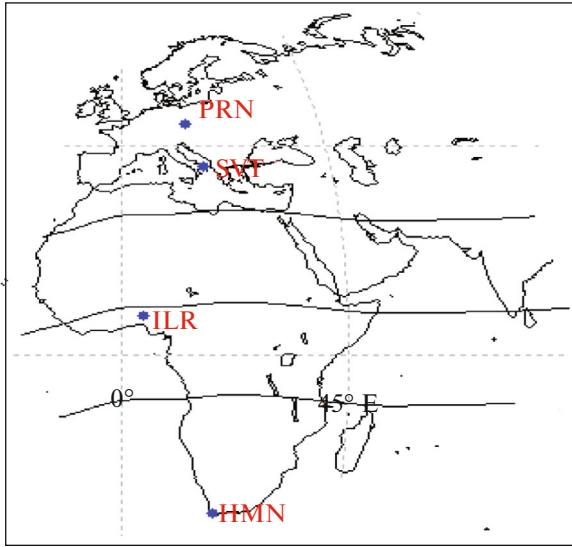


Fig. 1. Geographic location of the stations used.

The noon bite-out is a feature of the equatorial ionosphere. It is characterized by $NmF2$ depletions at/around noon, and $NmF2$ peaks occurring during the morning (Pre-noon peak) and afternoon (post-noon peak) hours. It is known to be driven by the dayside ExB upward drift (Lee, 2012). The strength of the bite-out was measured using the relationship in equation 2.

$$I_{br} = P_m - M_d \tag{2}$$

where I_{br} is the strength of the bite-out, P_m is the highest $NmF2$ value recorded either during the morning or afternoon hours and M_d is the minimum $NmF2$ value during the bite-out.

This in principle gives the measure of the effect of the ExB upward drift at a particular station around noon time.

3. RESULTS

3.1. Diurnal Variation of the Quietest Days $NmF2$ and $hmF2$

Figure 2, depicts the plot of the diurnal variation of (a) $NmF2$ and (b) $hmF2$ for the average ten quietest days of the months of May and August, 2010. These

months fall within the June Solstice and the September equinox seasons respectively.

Generally, it is known that the ionosphere usually starts building up at sunrise and then increases as the strength of solar radiation increases and decreasing sharply at sunset. Figure 2a reveals the differences in the (sunrise hour and) time of commencement of ionization in the Ionosphere. An observation from Fig. 2 shows that ionization begins earlier (at 0300 UT), and PRN, and begins around 0400 UT and 0500 UT at HMN and ILN respectively for the month of May. The time of commencement of ionization at ILN and HMN correspond during the month of August. Similar observation was also made for SVT and PRN during August 2010.

While the other stations (SVT, HMN and PRN) show multiple day time peaks of ionization, two clearly separated peaks of ionization (pre- and post-noon peaks) were noticed at ILN both during May and August. The quiet time $NmF2$ profile at SVT shows a unique feature compared to other stations, in spite of the multiple $NmF2$ peaks observed at SVT, two (one around sun rise and the other immediately after sunset) are most prominent and discernable both in May and August. Two peaks were also prominent at PRN, one at noon and the other immediately after sunset around 1900 UT.

The pre-noon peak at ILN was greater than the post-noon peak in May, and reverses in August. The minimum $NmF2$ for the daytime period observed (which occurred during the noon bite-out) at ILN coincides with that of SVT and PRN for the month of May. This was observed around 1300 UT and it also coincides well with the maximum $NmF2$ observed at HMN.

The maximum $NmF2$ values for the month of May and for each station occurred around the pre-noon period at ILN, post-noon period at HMN, and around the post-sun set period at PRN and SVT. Conversely, in the month of August, the maximum $NmF2$ values occurred during the post-noon period at HMN and around sunset at other stations. On the average, the rate of ionization is highest at ILN, followed by SVT, while it varies between HMN and PRN. The lowest $NmF2$ values of the day and night time recorded at HMN is an indication that the decay rate of ionization is faster at HMN when compared to the other stations. It begins with a sharp decrease in $NmF2$ around 14:00 UT at HMN, 1800 UT at ILN, 1900 UT and

Table 1. Record of Stations used for this study

S/No.	Station	Station code	Geographic		Geomagnetic		Local time
			latitude	longitude	latitude	longitude	
1	Pruhonice, Czech Republic	PRN	50.0° N	14.6° E	45.66° N	90.38° E	UT + 1
2	San Vito, Italy	SVT	40.4° N	17.8° E	34.68° N	87.13° E	UT + 1
3	Ilorin, Nigeria	ILN	8.5° N	4.5° E	1.87° S	76.67° E	UT + 1
4	Hermanus, South Africa	HMN	34.42° S	19.22° E	42.34° S	82.15° S	UT + 2

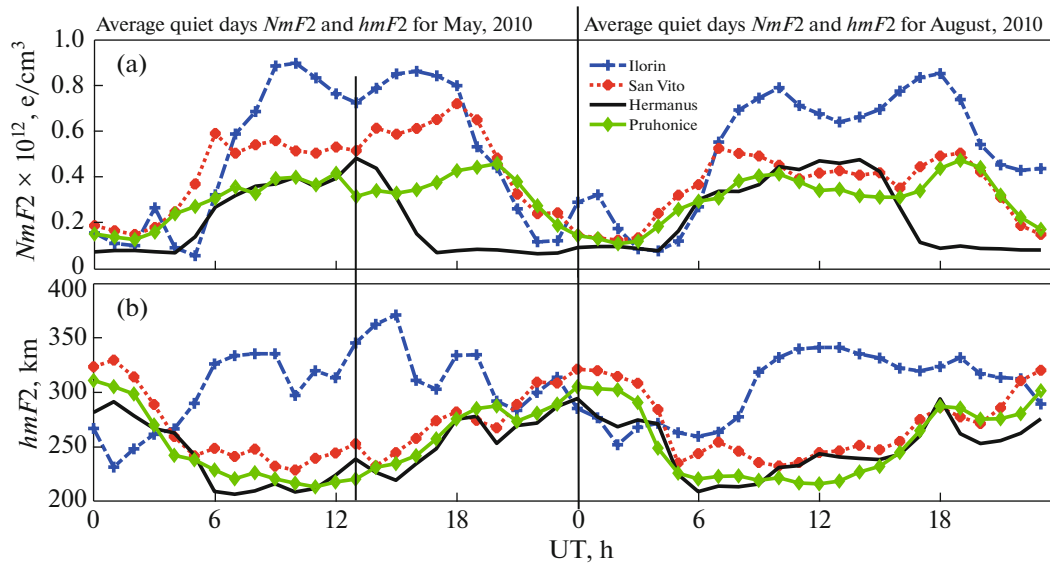


Fig. 2. Diurnal variations of the hourly averages of $NmF2$ and $hmF2$ values for the ten quietest days of the months of May and August.

2000 UT at SVT and PRN respectively both in the months of May and August. Post-midnight enhancement is mostly conspicuous at ILN, it appeared as $NmF2$ crest around 0300 UT and 0100 UT in May and August respectively.

Generally, it is known that the post-sunset Ionospheric $F2$ layer height is usually raised at the equatorial region as a result of the vertical plasma drift; this is clearly seen in the $hmF2$ morphology observed at ILN (Fig. 2b). It can be seen from this Figure that the maximum $hmF2$ values (of 371 km and 341 km in May and August respectively) for the daytime period occurred in ILN, followed by SVT and varies between HMN and PRN. On the average, the lowest $hmF2$ values for the daytime were recorded at HMN (about 209 km and 206 km in May and August respectively); this occurred during the buildup period (0600–0900 UT) of ionization in the ionosphere. Observations during the post sun-set and the night time period's shows higher $hmF2$ values at SVT, followed by PRN and lowest at ILN.

3.2. Storm Time Variation of the $F2$ -layer Electron Density and Peak Height During May 2, 2010 Geomagnetic Storm

Figure 3a shows (from top to bottom) the plot of IMF B_z and IEF E_y , Dst , solar wind speed (V_x), AE and AL indices and K_p index during the geomagnetic storm of 02 May, 2010. Figure 3b illustrates the time variation of (from top to bottom) Dst , $NmF2$ over ILN, SVT, HMN and PRN during the geomagnetic storm of 02 May, 2010. Figures 3c and 3d shows respectively $NmF2$ and $hmF2$ plots over ILN, SVT, HMN and PRN. The plots are from 30 April to 7 May, 2010. In

both plots the first panel shows the excursion of the Dst index. There was data gap at Ilorin on both $hmF2$ and $NmF2$ plots on 02 May.

3.2.1. $NmF2$ and $hmF2$ perturbations before the geomagnetic storm event. The IMF B_z experienced about 38 hours of southward orientation from 0600 UT on 30 April to 1900 UT on 01 May, 2010; with a slight enhancement in the IEF E_y (maximum value of about 0.79 mV/m around 1400 UT). During this period, the Dst and K_p indicated a quiet condition (minimum $Dst = -4$ nT, $K_p = 0.7$ all around 1600 UT), with an increase in the solar wind speed from 367 km/s at 1300 UT to a speed of about 395 km/s at 1600 UT. This coincides with the enhancement in $NmF2$ over ILN and HMN and depletion in SVT without any significant change at PRN, all on 30 April, 2010 as shown in Figures 3b and 3c. Considering the Dst and K_p values on this day, such major increase in $NmF2$ was not expected. This in principle points to the fact that Dst - and K_p -indices alone may not be sufficient to monitor geomagnetic disturbances. For instance the increase in the solar wind speed, the changes in the aurora indices, IEF E_y , as well as the southward B_z indicates the occurrence of an event that could have been responsible for the $NmF2$ perturbations. Similar observations were also made on 01 May, 2010.

3.2.2. Geomagnetic storm signatures and ionospheric responses. Panel 1 in Fig. 3a, showed that the IMF B_z turned northward around 1800 UT (after being southward for about 38 hours). This coincides well with the time of the SSC on May 1, thus indicating *the initial phase* of the storm. The IMF B_z turned from north (with a value of 8.5 nT at 0700 UT) to south reaching a minimum value of -8.2 nT at 1100 UT. This was further accompanied by several north-south epi-

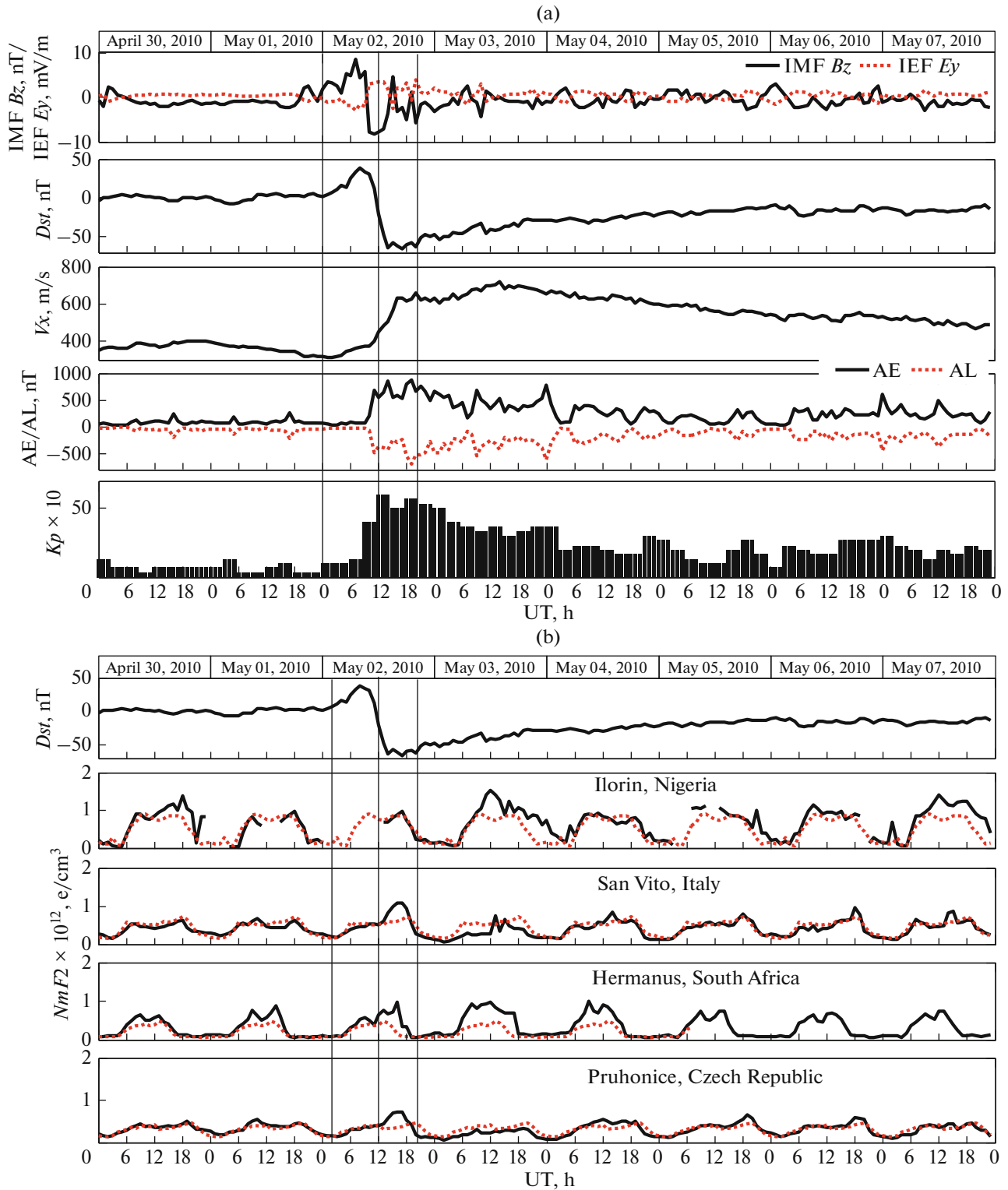


Fig. 3. (a) Diurnal variation of the interplanetary parameters (IMF B_z , IEF E_y), Dst , solar wind speed (V_x), Aurora indices (AL and AE), and K_p index, during the geomagnetic storm of 02 May, 2010; (b) The time variation of (from top to bottom) Dst , $NmF2$ over ILN, SVT, HMN and PRN during the geomagnetic storm of 02 May, 2010. The plot spans 30 April to 07 May, 2010. (The solid line represents the daily values and the broken line represents the quiet-time average); (c) The diurnal variation of (from top to bottom) Dst and the percentage change in $NmF2$ over ILN, SVT, HMN and PRN during the geomagnetic storm of 02 May, 2010. The plot spans 30 April to 07 May, 2010; (d) The diurnal variation of (from top to bottom) Dst and $hmF2$ over ILN, SVT, HMN and PRN during the geomagnetic storm of 02 May, 2010. The plot spans 30 April to 07 May, 2010. (The solid line represents the daily values and the broken line represents the quiet-time average).

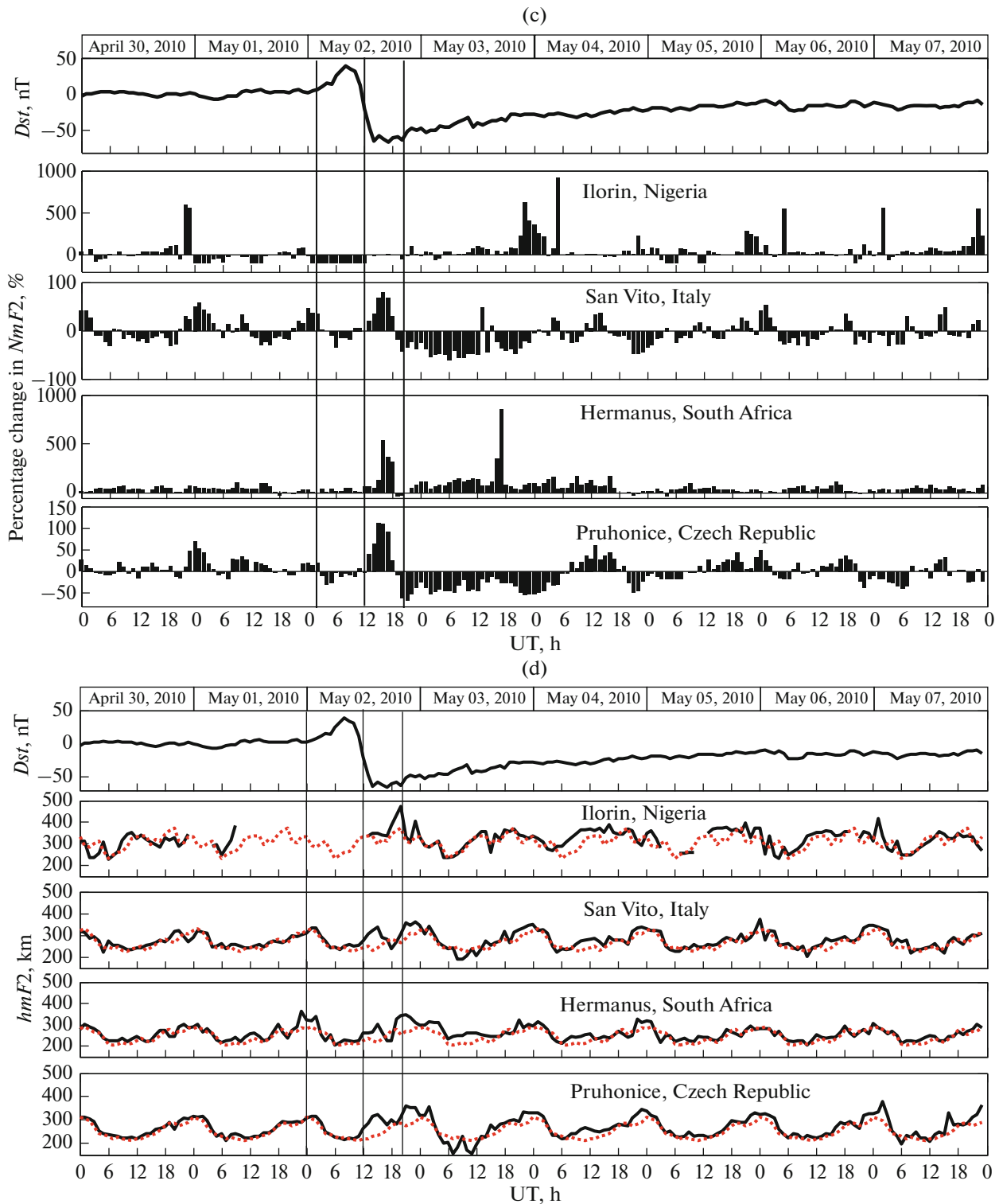


Fig. 3. (Contd.).

sodes of the IMF B_z . During this period, the solar wind speed increased significantly from 315 km/s to 662 km/s on 2 May. The increase in the solar wind speed was in agreement with the sharp decrease in the

Dst and the sudden rise in the aurora activity. This signaled the commencement of the *main phase* of the geomagnetic storm, which had three Dst excursions of -64 nT at 1400 UT, -66 nT at 1700 UT and -63 nT at

2000 UT, all on 2 May, 2010). While all the other indices reached their maxima during the main phase, the solar wind speed reached its maximum speed of about 700 km/s during *the recovery period* on 3 May, 2010.

In contrast to the *NmF2* and *hmF2* features of the quiet days (Figs. 2a, 2b), the geomagnetically disturbed period (Figs. 3b–3d) shows a deviation in terms of the *NmF2* and *hmF2* profiles from that of the quiet days. During the *initial phase*, both *NmF2* enhancement (46%) and depletions (–34%) were observed at SVT, 25% *NmF2* enhancement at HMN and 27% depletion in *NmF2* at PRN. There was no significant change observed during the initial phase in *hmF2* (Fig. 3d), except at HMN. However, day and nighttime *NmF2* enhancements otherwise known as Positive phase was discernible at all the stations except ILN, during the *main phase* of the geomagnetic storm. On the average, HMN recorded maximum *NmF2* enhancement (537%), followed by PRN (110%) and lowest at SVT (78%), these *NmF2* enhancements were observed to have lasted for over six (6) hours. There were data gaps at ILN around this period, thus making it difficult to properly analyze the change in *NmF2* during the main phase. However, depletion in *NmF2* (of about 51%) that is consistent with an increase in *hmF2* was evident on that day (Figs. 3c, 3d) at ILN.

A major *NmF2* enhancement/Positive phase (with a duration that is greater than 12 hours) was discernible at ILN (916%) and HMN (850%) respectively, while a negative phase of over 30 hours was dominant at SVT (–47%) and PRN (–55%) during the *recovery phase* on May 3, 2010. These observations correspond well with the increases in the peak height on that day across the stations. While the maximum *NmF2* enhancement for ILN and HMN occurred during the recovery period that of PRN and SVT was observed during the main phase of the geomagnetic storm.

3.3. Storm Time Variation of *NmF2* and *hmF2* During the Geomagnetic Storm of May 28–29, 2010

3.3.1. Geomagnetic storm signature. From top to bottom of Fig. 4a depicts the temporal variation of the IMF B_z and IEF E_y , *Dst*, solar wind speed (V_x), AE and AL indices and *Kp* index during the geomagnetic storm of 02 May, 2010. Figure 4b shows the time variation of (from top to bottom) *Dst*, *NmF2* over ILN, SVT, HMN and PRN. Figures 4c and 4d, illustrate respectively the percentage change in *NmF2* and *hmF2* plots over ILN, SVT, HMN and PRN. On both Figures, the first panel shows the time variation of the *Dst* index. The plots span 27 May–02 June, 2010 to cover at least one quiet day before the commencement of the geomagnetic storm.

From Figures 4a, it is evident that *the initial phase* of the geomagnetic storm began on 28 May at 0100 UT with an SSC. The solar wind speed was observed to increase from 317 km/s (0100 UT) to 385 km/s

(0900 UT) and remained at this value through the day. This increase was simultaneous with the rise in *Dst* index values from 2 nT (at 0200 UT) to 28 nT (at 0900 UT), as well as a northward turning of the IMF B_z on 28 May, 2010. Several episodes of northward and southward orientation of the IMF B_z and a flux in *Dst* were observed between 0100–1900 UT on the same day.

The southward turning of the IMF B_z around 1900 UT on 28 May, that lasted for about 12 hours (from 19 nT at 1900 UT on 28 May to –14 nT at 0600 UT on 29 May) signaled the commencement and development of the *Main Phase* of the geomagnetic storm. It has been shown earlier by Kane, (2005) that the duration for which the IMF B_z experienced a southward orientation is vital in the geomagnetic storm occurrence. An increase in the IEF E_y reaching its maxima (4.86 mV/m) around 1100 UT on 29 May. The *Dst* index attained its minimum value (–84 nT) at 1200 UT. *Kp*, AE and AL indices respectively attained their maximum values of 53, 1268 nT and –892 nT, simultaneously with the *Dst* index.

3.3.2. *NmF2* and *hmF2* perturbations observed before geomagnetic storm. Figures 4b and 4c shows *NmF2* and *hmF2* perturbations (enhancement/depletion) on 27 May, 2010 before the SSC. These perturbations appeared as a decrease in the pre-noon peak as well as an increase in the *NmF2* post-noon peak at ILN. A decrease in the *NmF2* post-noon peak at HMN, SVT and PRN, and was consistent with *hmF2* deviations. These *NmF2* perturbations occurred during the geomagnetically quiet period (based on *Dst* and *Kp* indices), with minimum *Dst* of 0 nT and *Kp* = 13. However, a slight increase of about 20 (from 345 to 362) km/s in the solar wind speed was observed prior to the commencement of these *NmF2* and *hmF2* perturbations. This occurred around 0200–0600 UT and thereafter began to decrease. The IMF B_z was observed to have experienced a southward excursion around 08:00–1500 UT the same day. During this period there was an enhancement of the IEF E_y (0.76 mV/m) which coincides well with the southward IMF B_z (at –2.2 nT) and the maximum value of the AE (131 nT) for this day, all occurring around 1000 UT.

3.3.3. Storm time variation of *NmF2* and *hmF2*. An observation from Figs. 4b and 4c reveals a marked variation from that of the average quiet days in the month of May as discussed earlier in Fig. 2. *NmF2* variations that appeared either as enhancements or depletions were observed during the daytime (i.e. 0600–1800 UT) and nighttime (1900–0500 UT) on disturbed days. During the *initial phase* (SSC), depletion in *NmF2* of about 86% and 48% was observed at ILN and HMN respectively. While this *NmF2* depletion affected the entire daytime period at HMN, it affected the pre-noon period only at ILN. Both *NmF2* enhancement and depletions of about 40% were observed at SVT, while *NmF2* enhancement of about 65% was recorded at PRN.

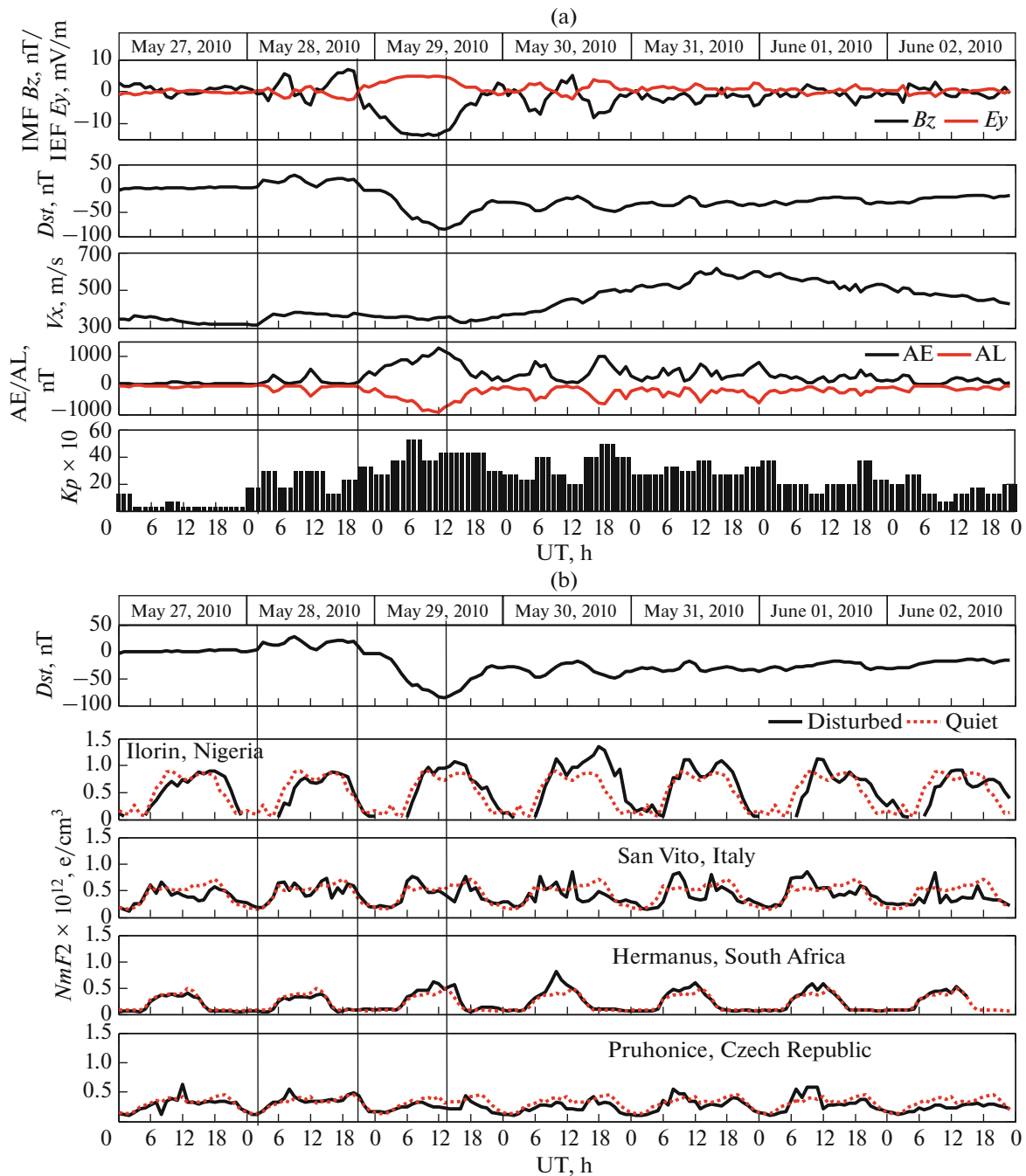


Fig. 4. (a) Diurnal variation of (Top to bottom); IMF B_z and IEF E_y , Dst , solar wind speed (V_x), Aurora indices (AL and AE), and K_p index, for the geomagnetic storm of 28–29 May, 2010. The plot covers the period of 27 May to 02 June, 2010; (b) The time variation of (from top to bottom) Dst , $NmF2$ over ILN, SVT, HMN and PRN for the geomagnetic storm event of 28–29 May, 2010. The plot is for 27 May to 02 June, 2010. (The solid line represents the daily values and the broken line represents the quiet-time average); (c) The diurnal variation of (from top to bottom) Dst and the percentage change in $NmF2$ over ILN, SVT, HMN and PRN for the geomagnetic storm of 28–29 May, 2010. The plot extends from 27 May to 02 June, 2010; (d) The diurnal variation of (from top to bottom) Dst and $hmF2$ over ILN, SVT, HMN and PRN for the geomagnetic storm event of 28–29 May, 2010. The plot covers 27 May to 02 June, 2010. (The solid line represents the daily values and the broken line represents the quiet-time average).

$NmF2$ experienced both enhancements and depletion during the **main phase**. Figures 4b and 4c show prominent cases of $NmF2$ depletion of about 54% and 39% at ILN and PRN respectively; while $NmF2$ over SVT experienced both enhancement and depletion of

about 53% and 50% respectively. The maximum $NmF2$ enhancement for this phase occurred at HMN (81%). However, as the Dst index began to recover from its minimum excursion (around 1400 UT on 29 May, 2010), signifying the commencement of the

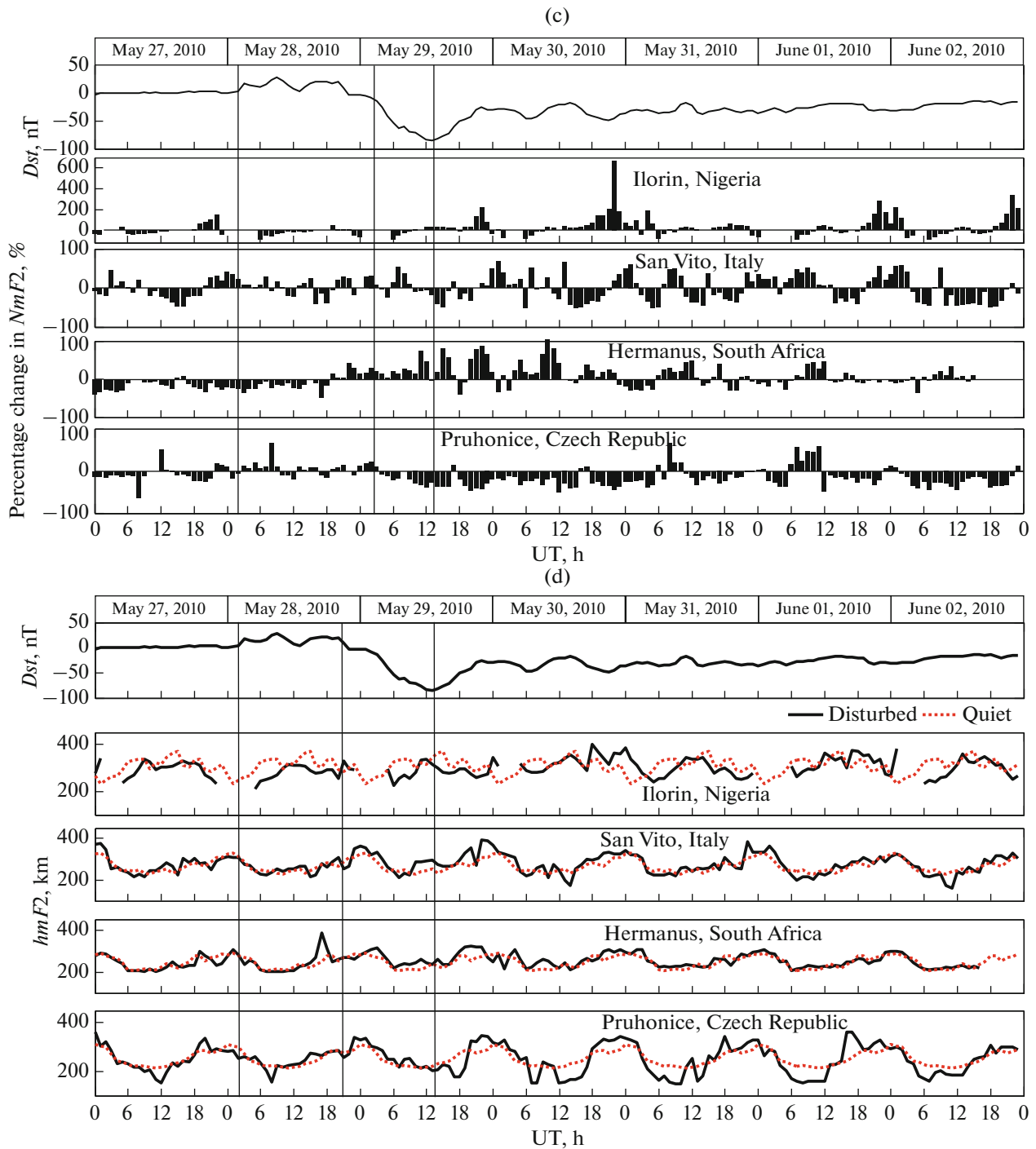


Fig. 4. (Contd.).

recovery phase; *NmF2* enhancements were recorded at all the stations except PRN. As the **recovery phase** progresses, a prominent increase in *NmF2* was recorded at ILN and HMN with a percentage deviation of about 674% (around 2200 UT) and 103% (1000 UT) respectively on 30 May, 2010. Two distinct peaks of ionization were observed at ILN on 30 May. First *NmF2* peak was observed around 1000 UT and it corresponds

well with the single *NmF2* peak observed at HMN the same day. It was also observed that the second peak at ILN corresponds well with the *NmF2* depletion observed at SVT and PRN on the same day.

These *NmF2* features observed at ILN during the recovery period are similar to the quiet time *NmF2* morphology, featuring the noon bite-out with two clearly separated *NmF2* peaks, one each during the

pre-and post-noon periods, with $NmF2$ depletion around noon time. However, the bite-out occurred earlier during geomagnetic storms, when compared with that of the quiet time averages in Fig. 2a. Unlike what was observed on the quiet time $NmF2$ morphology, the post-noon peak was greater than the pre-noon peak during the geomagnetic storms. The intensity of the bite-out during geomagnetic storms (a difference of about $0.5252 \times 10^{12} \text{ e/cm}^3$, about 63%) was also observed to be higher than that of the quiet time averages (a difference of about $0.1724 \times 10^{12} \text{ e/cm}^3$, about 24%). This indicates that the geomagnetic storm led to the enhancement of the bite-out.

Figure 4d shows a decrease in $hmF2$ recorded at ILN during the initial, main and the early part of the recovery period of the geomagnetic storm (i.e. 28–29 May). However, as the recovery phase progresses, there was an increase in $hmF2$ which was observed to be consistent with the prominent $NmF2$ enhancement observed at ILN on 30 May 2010. Increases in $hmF2$ were dominant at SVT and HMN during all phases of the geomagnetic storm, while both $hmF2$ increases and decreases were evident at PRN.

3.4. Storm Time Variation of the F2-layer Peak Parameters during the Geomagnetic Storm Event of August 3–4, 2010

Figure 5a shows (from top to bottom) the plot of the diurnal variation of the IMF B_z and IEF E_y , Dst , solar wind plasma speed (V_x), AE and AL indices and K_p index during the geomagnetic storm of 03–04 August, 2010. Figure 5b shows the diurnal variation of (from top to bottom) Dst , $NmF2$ over ILN, SVT, HMN and PRN. Figures 5c, 5d shows respectively the percentage change in $NmF2$ and $hmF2$ plots over ILN, SVT, HMN and PRN. In both plots, the first panel shows the variation in the Dst index. The plots span 02–07 August, 2010, to cover at least one quiet day before the commencement of the geomagnetic storm.

3.4.1. Pre-storm time features of $NmF2$ and $hmF2$.

An observation from Fig. 5b reveals distinct $NmF2$ and $hmF2$ perturbations before the SSC on August 2. While the perturbations occurred as a decrease in the $NmF2$ pre-noon peak at ILN and HMN (about 44 and 51%, respectively), they were seen as enhancements in the pre-noon peak at SVT (about 104%). The Dst had a minimum value of -6 nT on that day, while the AE index was observed to have increased from 97 to 242 nT within 5 hours (from 1000–1500 UT). There were several episodes of North-Southward orientation of the IMF B_z on the same day. However, it was observed that the IMF B_z was southward during the observed changes in the $NmF2$. Slight enhancements and depletions in the IEF E_y were also evident the same day.

3.4.2. Geomagnetic storm signature and ionospheric responses. Figure 5a shows that the geomagnetic storm began with *an initial phase* that is characterized by a

gradual increase in the Dst index from -12 nT (at 0500 UT) to 05 nT (at 1600 UT) on 03 August, 2010. This was accompanied by a sharp rise in Dst to a value of 20 nT (at 1900 UT), which happened together with the abrupt rise in the solar wind speed from 406 km/s (at 1500 UT) to 581 km/s at 1900 UT. During this period there was also a sharp northward turning of the IMF B_z to a peak value of 9.3 nT , and was observed to be simultaneous with the reduction observed in the IEF E_y to a minimum value of -5.24 mV/m both occurring around 1800 UT. This led to a decrease in $NmF2$ at ILN (about -75%) and PRN (about -37%), both $NmF2$ enhancement (about 37%) and depletion (about 65%) at SVT, and $NmF2$ enhancement at HMN (65%) all on 3 August, as shown in Figs. 5b, 5c.

After the SSC, at about 1900 UT, a number of events of north-southward IMF B_z and increases/decreases in IEF were clearly seen around 1900 UT on 03 August to 0200 UT on 04 August, as shown in Fig. 5a. Manju et al. (2009) has earlier shown that during these incidents of north-southward IMF B_z , the prompt penetration of the interplanetary electric fields (IEF) into the equatorial/low and mid latitude ionosphere usually takes place. This in principle can lead to the alteration of the quiet time zonal electric field, thus leading to the observed changes in the equatorial and low latitude ionosphere.

The subsequent decrease in the Dst immediately after the SSC, signifies *the Main phase* of the storm that had two minimum negative values of -63 nT at 2300 UT on 3 August, and -67 nT at 0400 UT on 4 August. Both Dst minimum excursions coincides well with the maximum value of the solar wind speed (about 600 km/s) for the period. During this period, observations from Figs. 5b, 5c show $NmF2$ enhancements at HMN, SVT and ILN (although there were data gaps at ILN) while $NmF2$ depletions were recorded at PRN. On the other hand, Fig. 5d shows increases in $hmF2$ across all the stations during this period.

The increase in the Dst index that started at about 0400 UT on 04 August, is indicative of the commencement of the recovery phase of the geomagnetic storm event. At the commencement of this recovery phase, the IMF B_z turned northward, reaching a peak value of 14.1 nT at 0700 UT which was simultaneous with the minimum depression of the IEF E_y (about -8.11 mV/m , around 0700 UT) for the entire period as shown in Fig. 5a. However, shortly after the geomagnetic storm began to recover; the IMF B_z suddenly turned southward again and had a minimum excursion of -6.1 nT , which coincided with an enhanced value of the IEF E_y of about 3.25 mV/m both occurring around 1700 UT on 04 August, 2010. The IMF B_z remained southward for over 12 hours. Daglis, (1997), have shown that during the recovery period of some geomagnetic storms, injection of new energetic particles usually occur into the Earth's mag-

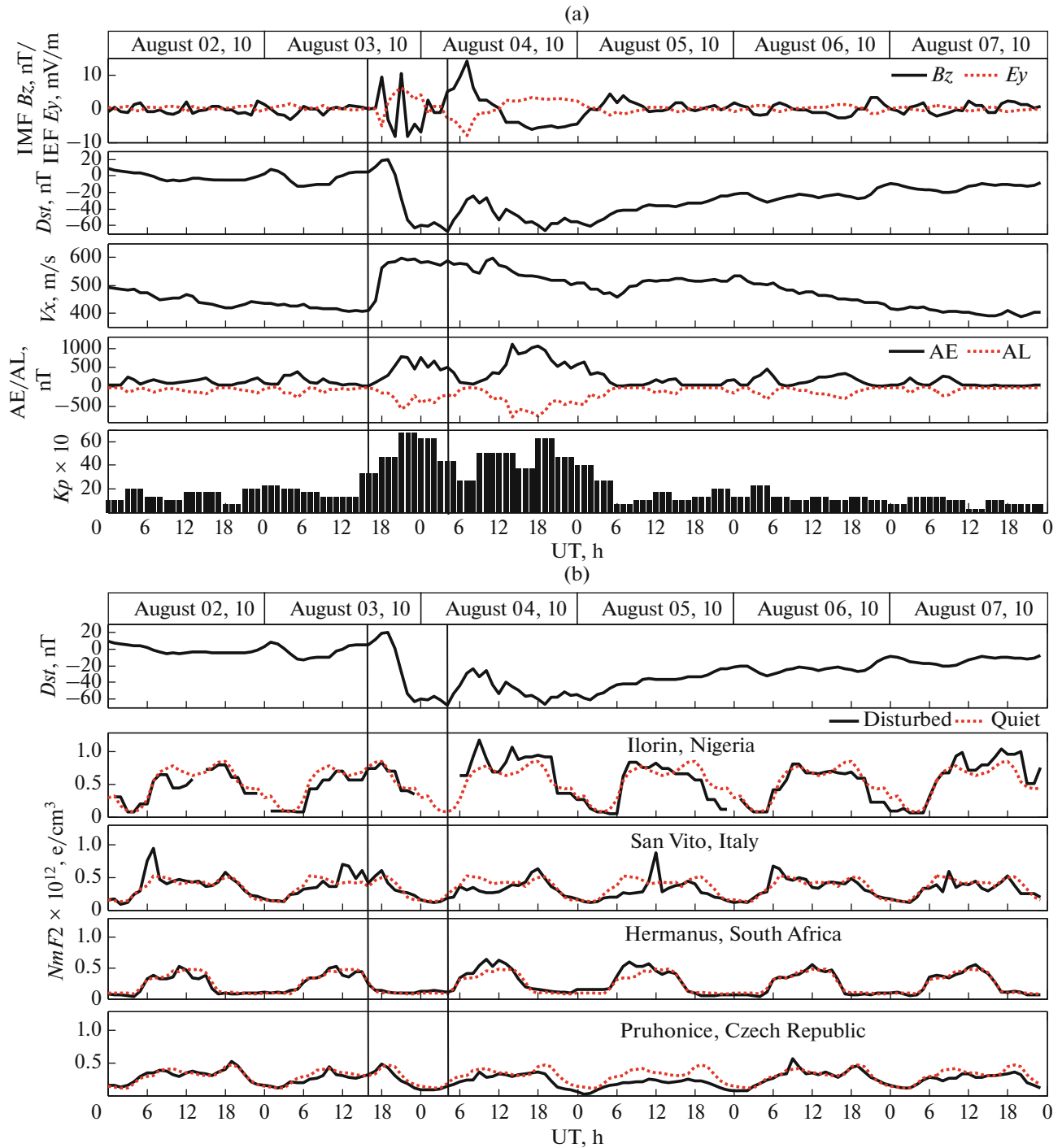


Fig. 5. (a) Diurnal variation of the (top to bottom); IMF B_z and IEF E_y , Dst , solar wind speed (V_x), AL and AE, and K_p index, during the geomagnetic storm of 03–04 August, 2010. The plot covers 02–07 August, 2010; (b) The time variation of (from top to bottom) Dst and $NmF2$ over ILN, SVT, HMN and PRN during the geomagnetic storm of 03–04 August, 2010. The plot is for 02–07 August, 2010. (The solid line represents the daily values and the broken line represents the quiet-time average); (c) The diurnal variation of (from top to bottom) Dst and the percentage change in $NmF2$ over ILN, SVT, HMN and PRN during the geomagnetic storm of 03–04 August, 2010. The plot covers the period of 02–07 August, 2010; (d) The diurnal variation of (from top to bottom) Dst and $hmF2$ over ILN, SVT, HMN and PRN during the geomagnetic storm of 03–04 August, 2010. The plot covers the period of 02–07 August, 2010. (The solid line represents the daily values and the broken line represents the quiet-time average).

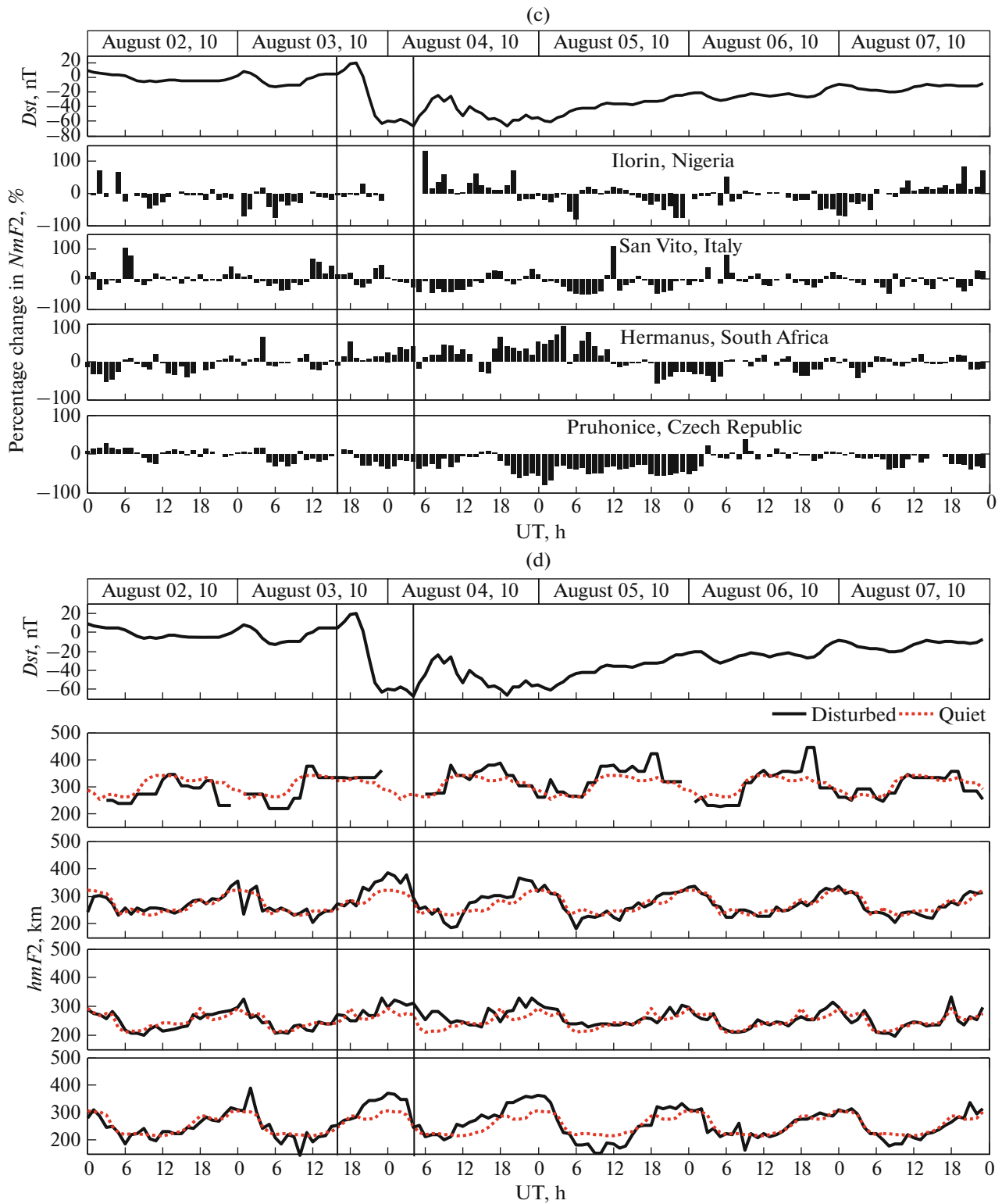


Fig. 5. (Contd.).

netosphere. Thus, causing an increase in the ring current that usually leads to a further decrease in the Dst index. This is evident with the sudden rise in the

plasma speed of 54 km/s recorded within 3 hours (from 0800–1100 UT) and is consistent with the commencement of the depression in the Dst index on

04 August. The Dst Index decreased gradually and had three different negative excursions; -53 nT at 1200 UT, -66 nT at 1900 UT both occurring on 04 August and -61 nT at 0200 UT on 05 August (Fig. 5a). The last two out of the three *Dst* excursions happened at night, when the ionization is usually low in the ionosphere. Further observations from this Figure, also shows a marked increase in the aurora indices during this period (AE had an increase of 1.038 nT in 6 hours, while, AL decreased by 748 nT in 7 hours).

Consequently, a considerable Positive phase with two clearly separated peaks was evident at ILN and HMN, a single *NmF2* peak at SVT and majorly *NmF2* depletion at PRN on 04 August. The first peak at ILN and HMN occurred around 0900 UT and 1000 UT respectively, coinciding well with the time the IMF *Bz* suddenly turned northward. The second peak on the other hand, was noticed around 1400 UT and 1200 UT, respectively at ILN and HMN. The second peak at HMN was consistent with the time ILN experienced a daytime minimum. Figure 5b further shows that ILN recorded a higher pre-noon peak than that of the post-noon period on this day (04 August) in contrast to the quiet time observations; the magnitude of the bite-out was also observed to be greater than that of the quiet days.

The multiple peaks that were observed in the average quiet time plots were compressed into two distinct peaks at HMN during geomagnetic storms. The *NmF2* observations at SVT during this period show an enhancement of the pre-noon peak, while results from PRN show depletion in *NmF2* although with about three peaks of ionization. Night time *NmF2* depletions were also observed around this period at HMN and PRN, both occurring during the post mid-night period.

On the other hand, Fig. 5d reveals that the recovery phase of this geomagnetic storm was characterized by *hmF2* increases at all stations. The *hmF2* plots at ILN show two peaks with each corresponding to one of the *NmF2* peaks observed in Fig. 5b on 04 August. Although, the *hmF2* values were less than 400 km during the initial and main phases of the geomagnetic storm, the maximum value of *hmF2* (450 km) occurred on 6 August during the post-noon period and was consistent with the decrease in *NmF2* observed on that day.

4. DISCUSSION

The *NmF2* and *hmF2* responses to some geomagnetic storm events that occurred in 2010 has been examined using the Digisonde observations from one equatorial station (ILN), and three mid-latitude stations (HMN, SVT and PRN). These four stations fall within a close range of longitude and as such, have the same local time, except for HMN that is one hour ahead. Considering the geographic coordinates, ILN, SVT and PRN fall within the northern hemisphere, while HMS falls in the southern hemisphere. How-

ever, considering their geomagnetic coordinates, ILN and HMN fall in the southern hemisphere. This may partly account for some of the similarities observed in the responses of the two stations during geomagnetic storms.

4.1. Average Quiet Days Observations

Generally, it is known that the movement of ionization in the ionosphere is been controlled by the universal system of currents, electric fields, neutral winds and chemical processes (Sastri, 2006). These factors are known to determine the global distribution of the ionospheric plasma.

The quiet time morphology of the *NmF2* over Ilorin is characterized by two peaks of ionization that usually occur during the morning and post noon period, with *NmF2* depletion (bite-out) around noon. This *NmF2* depletion is known to be driven by the ExB vertical drift during the daytime. It was also observed that the minimum *NmF2* for the daytime period observed during the bite-out at ILN coincides well with the maximum *NmF2* observed at HMN occurring around 1300 UT (although HMS is one hour ahead of ILN). This is indicative of the movement of electrons from the equatorial ionosphere to the higher latitudes around this time, and causing *NmF2* depletions at the equatorial region by the fountain effect. This is possible, since the two stations fall within the same hemisphere, though at different latitudinal regions based on their geomagnetic coordinates.

Other major quiet time findings such as the high rate of ionization observed at ILN, the low values of *NmF2* at other stations and the high rate of decay of ionization observed at HMN can be associated with the ionospheric dynamics that exist at different latitudinal region (Fejer et al., 1983). The intensity of the ionizing solar radiation that varies across the latitudes is also a major contributing factor to the variation of *NmF2* across the latitudes. It is known that the angle of arrival of the ionizing solar radiation is directly above the equator and tilted away from the equator. This accounts for the higher values of *NmF2* around the equatorial and low latitude region.

The highest *hmF2* peaks (371 km and 341 km in May and August respectively) observed at Ilorin during daytime also suggest the lifting of the ionospheric *F2* layer at that region by the fountain effect. This can also lead to a reduction in the recombination rate and thus giving rise to the higher *NmF2* values observed at this station.

4.2. Storm-time Variation of *NmF2* and *hmF2*

Interestingly, the *initial phase* of the three geomagnetic storms had sudden storm commencement (SSC). During this phase, it was observed that the IMF *Bz* rapidly changes its direction either from north to south or vice versa. This usually affects the polarity

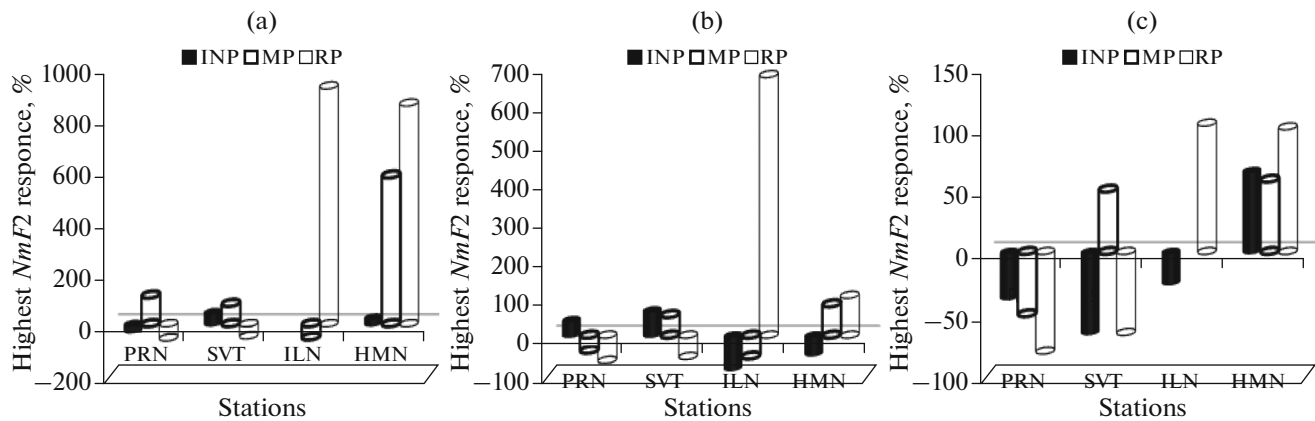


Fig. 6. Statistical distribution of the F2 layer response to (a) 02 May, (b) 28–29 May, and (c) 03 August, 2010 geomagnetic storms. There were data gaps at ILN during the 02 May, and 03 August geomagnetic storms. The statistics represent highest percentage values recorded during each phase.

of the interplanetary electric field, giving rise to fluctuations in the vertical drift of the F layer (Manju et al., 2009). Adeniyi (1986) has earlier shown that during an SSC, enhancements in the ExB drift usually occur, which results in $NmF2$ depletions at the equatorial region. This explains the cases of decreases in $NmF2$ observed in ILN that were also consistent with the decrease in $hmF2$ during the initial phase. Interestingly, this study also recorded cases of depletions at the mid-latitudes during the initial phase of the geomagnetic storms, as shown clearly in Fig. 6. This Figure shows the statistical representation of the $NmF2$ responses from each station and at different Phases.

$NmF2$ responses on 30 May and 04 August observed at ILN, shows an increase in the magnitude of the noon bite-out during geomagnetic storms. There was also an adjustment in the time of occurrence of the bite-out by the geomagnetic storm event. It is clearly seen that the bite-out occurred earlier during the disturbed days when compared to that of the quiet days. These kinds of observations were also earlier reported by some studies (Lastovicka, 1996, Burns et al., 2007, Olawepo and Adeniyi, 2012) from the equatorial and low latitude region. This is as a result of alterations of the quiet time ExB force by the geomagnetic storms. It was also observed that, while ILN experienced noon-time depletion, HMN recorded an enhancement around that same time during the two geomagnetic storm events. Although two $NmF2$ peaks were also recorded at HMN on 04, August, the first peak occurred when ILN experienced its midday minimum. However, maximum $NmF2$ enhancement for all the stations is mostly recorded during the recovery period of the geomagnetic storms (both in May and August) as shown in Fig. 6. It can be deduced further from Figure 6 that while ILN and HMN show a prominent case of a positive storm effect ($NmF2$ enhancements) during the recovery periods, SVT and PRN show negative storm effect ($NmF2$ depletions). Aver-

agely, Positive storm effect is observed to be prevalent at HMN and SVT (except for August 3, storm event), the negative storm effect is dominant at PRN during the three geomagnetic storms. This cannot be unconnected with the latitudinal position of the stations, thus indicating an increase in the likelihood of having negative storm effect with the increase in geomagnetic latitude. Fejer (1991) has earlier shown that ionospheric storms are usually been driven by certain factors such as: the intensity of the geomagnetic storm, latitudinal position, local time of the stations, season of the year, and solar activity.

The $NmF2$ response observed at the mid-latitudes can be attributed to the changes in the global thermospheric circulation as a result of the pressure gradient that develops during geomagnetic storms (Bounsanto, 1999). It is generally known that Joule heating usually occurs at the auroral region during all classes of geomagnetic storms. This joule heating alongside the particle precipitation usually results in the upwelling of the Atmosphere around the auroral oval (Zhang et al., 2004, Sur et al., 2019). Mayr and volland, (1972) has earlier shown that the upwelled atmosphere contains less number of ionized oxygen with a significantly high amount of neutral nitrogen molecules, that are been transported by the meridional neutral wind towards the mid- and low- latitudes. These is responsible for the decrease in the ionospheric electron density (Zhang et al., 2004) in the mid- and low latitude region particularly during the main and the recovery phases of the geomagnetic storms.

Figure 7 shows the Global Ultraviolet Image (GUVI) of the ratio of the O/N_2 for 30th April to 05 May, 2010. Considering 30th April, 2010 as a reference for a typical quiet day, it could be seen clearly that there was an enhancement in the O/N_2 ratio that started at the southern aurora/High latitude during the main phase of the storm on 02 May, 2010. The enhancement and depletion (as seen in the Northern

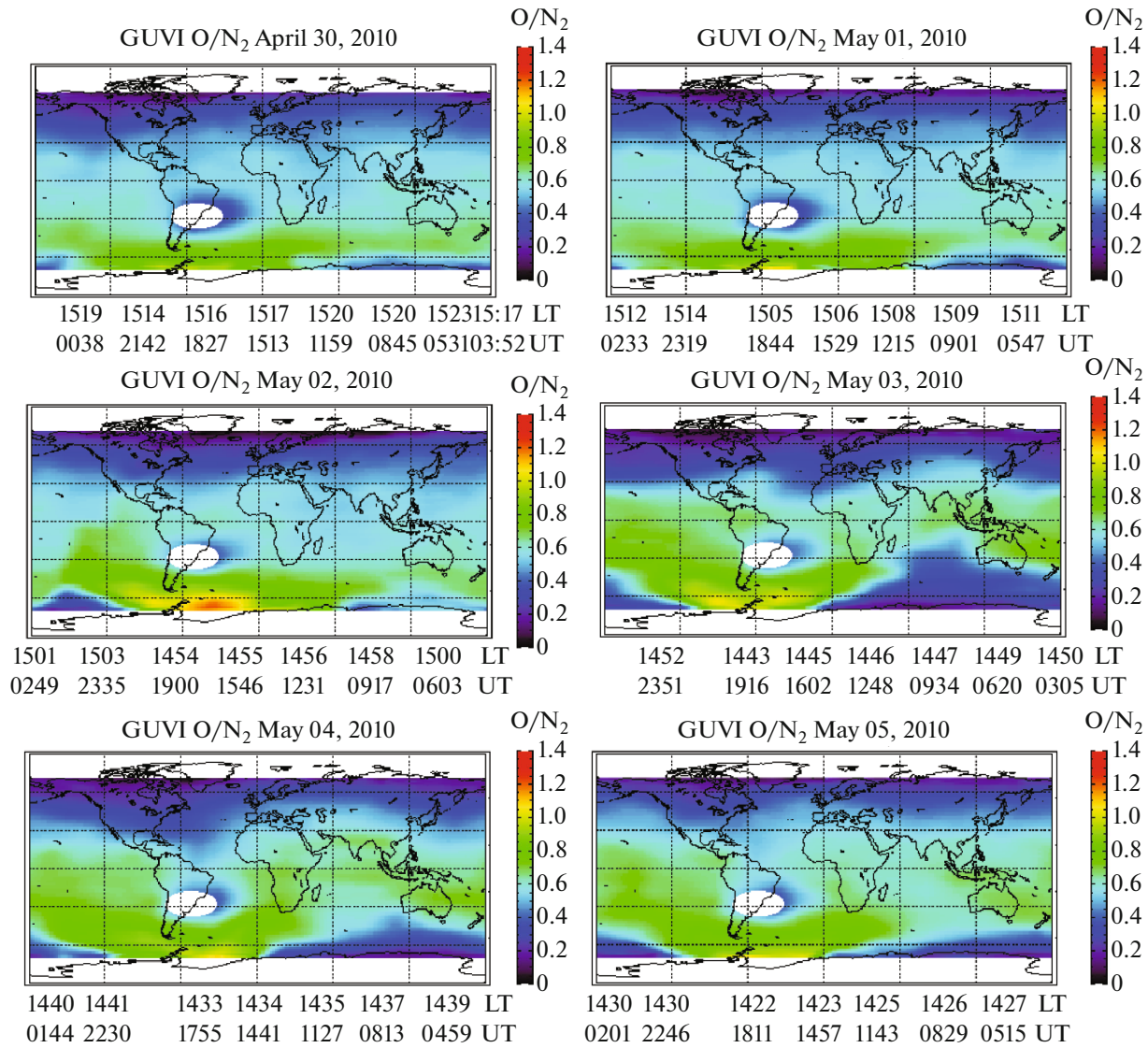


Fig. 7. O/N₂ ration global maps for 30 April to 05 May, 2010 obtained from the Global Ultraviolet Imager (GUVI) website.

aurora/high latitude in the figure) in O/N₂ ratio is indicative of its regional and global behavior that is usually observed during geomagnetic storms (Habarema, 2013) as it corotates the Earth (Zhang et al., 2004). This enhancement in the O/N₂ ratio was observed to have spread gradually into the mid- and low latitudes in the southern hemisphere, through 03–05 May, 2010. This could have led to the strong positive storm effect observed in HMN, a mid-latitude station on 02–03 May, 2010. Astafyeva et al. (2015) has earlier pointed out that one of the unpredictable features of the ionospheric response to geomagnetic storms is the *NmF2* enhancement in the mid-latitudes. This can be observed in the case of PRN, where we observed a prominent negative storm effect during the main and recovery phases of all the geomagnetic storm

events considered, except during the main phase of May 02, geomagnetic storm.

5. SUMMARY OF FINDINGS

The ionospheric response to three geomagnetic storms during May and August, 2010 has been examined using *NmF2* and *hmF2* data obtained over four Digisonde stations. These stations were located along a close range of longitude; they include one equatorial station of Ilorin and three mid-latitude stations (Hermanus in the African sector, San Vito in Italy and Pruhonice in the Czech Republic). The aim of the study was to investigate study the latitudinal dependence in the ionospheric responses to geomagnetic storms. The results of the study are summarized below.

i. The quiet time observations show that the rise in $NmF2$ began earlier at the mid latitude stations of SVT and PRN. However, the rate of ionization is highest at Ilorin an equatorial station, while the rate of decay/collapse on $NmF2$ was observed to be higher at HMN. Post-midnight enhancement is mostly conspicuous at ILN, it appeared as $NmF2$ crest around 0300 UT and 0100 UT in May and August respectively.

ii. While the other stations (SVT, HMN and PRN) show multiple daytime peaks of ionization, two clearly separated peaks of ionization were observed at ILN both in May and August. This $NmF2$ morphology around Ilorin (the noon bite-out) is attributed to the fountain effect.

iii. Maximum $hmF2$ values (about 371 km and 341 km in May and August respectively) for the daytime period occurred in ILN, followed by SVT. The highest values of $hmF2$ observed at Ilorin further reveals the lifting of the ionospheric $F2$ layer by the fountain effect.

iv. The $NmF2$ and $HmF2$ perturbations observed during the quiet days before the SSC are indicative of a need to critically reconsider the quiet time definitions to capture changes in the aurora indices, solar wind plasma speed and IMF Bz .

v. During the geomagnetically disturbed condition, the $NmF2$ features at Hermanus and Ilorin show lots of similarities, though the duo are from different latitudinal region. Both $NmF2$ enhancement and depletions were both observed at all stations, with the maximum enhancement occurring at Ilorin, followed by Hermanus, the least is Pruhonice. However, depletions are mostly prominent at Pruhonice.

vi. Long hours (>6 hours) of $NmF2$ enhancements were observed at all the mid latitude stations (SVT, HMN and PRN) during the main phase of the 02 May, 2010 geomagnetic storm, with no any noticeable change over ILN a station in the equatorial latitude. Similar observation was also made at ILN and HMN (long time duration of $NmF2$ enhancement >12 hours) during the recovery phase; while that of HMN occurred during the daytime alone, it was across both day and night time at ILN. $NmF2$ depletions for over 30 hours which coincides well with increases in $hmF2$ were dominant at PRN and SVT during this phase.

vii. For recovery periods, both $NmF2$ enhancement and depletions were common at SVT, $NmF2$ depletions at PRN and prominent features of $NmF2$ enhancement dominate ILN and HMN. While ILN and HMN records maximum enhancements during the recovery periods, SVT and PRN recorded theirs during the main phases of the geomagnetic storms.

viii. A simultaneous enhancement in $NmF2$ at ILN and $NmF2$ depletion at SVT and PRN were also recorded during geomagnetic storms.

ix. In contrast to the noon bite-out observed during geomagnetically quiet conditions, the post-noon peak was observed to be higher than the pre-noon peak

during the geomagnetic storms. The intensity of the bite-out during geomagnetic storms was also observed to be higher than that of the quiet time averages by about 40%.

6. CONCLUSIONS

It is evident from this study that although all the geomagnetic storms were moderate geomagnetic storms, yet the ionospheric responses vary with time of occurrence of the geomagnetic storm, season and latitudinal location of the station as earlier reported by many recent and previous studies. Earlier works (Adeniyi, 1986, Lastovicka 1996, radicella and Adeniyi, 1999, Buonsanto, 1999, Burns et al., 2007, Adebesein, 2008, Olawepo and Adeniyi, 2012, Adekoya et al., 2012 and many more) have reported latitudinal differences in the ionospheric responses to geomagnetic storms. These studies indicated $NmF2$ depletions at the high and mid latitude and $NmF2$ enhancement at the equatorial and low latitudes. It is however, evident from this study that ILN an equatorial station and HMN in the mid latitude show similar responses to the geomagnetic storms particularly during the recovery phase. Also, positive storm effect is prevalent at ILN, HMN and SVT, while the negative storm effect is dominant at PRN during the three geomagnetic storms. This suggests a likelihood of having negative storm effect with the increase in geomagnetic latitude during geomagnetic storm events. The responses of the stations to the initial phase of the geomagnetic storms vary from station to station and also with the duration of the SSC.

ACKNOWLEDGMENTS

We thank the organizing committee of the first Varsity symposium 2016, for the invitation and financial support to attend the conference, where this work was first presented as a poster.

We also appreciate the management and administration of all the observatories that made available the data used in this study.

The authors also wish to acknowledge the support and contributions of Dr. Huixin Liu of the Department of Earth and Planetary Science, Kyushu University, Japan.

The contribution and efforts of the anonymous reviewers of this paper and the editor of this journal is quite appreciated and commendable.

FUNDING

This study was not funded by any organization or agency.

REFERENCES

- Adebesein, B.O., F2 region response to the magnetic storm of January 10, 1976 at American Sector, *Afr. Phys. Rev.*, 2008, vol. 2, pp. 136–142.

- Adebesin, B.O. and Chukwuma, V.U., On the variation between D_{st} and IMF B_z during ‘intense’ and ‘very intense’ geomagnetic storms, *Acta Geod. Geophys. Hung.*, 2008, vol. 43, pp. 1–15.
<https://doi.org/10.1556/AGeod.43.2008.1.1>
- Adebiyi, S.J., Adeniyi, J.O., Adimula, I.A., Joshua, B., and Gwani, M., Effect of the geomagnetic storm of April 5–7, 2010, on the F2-layer of the ionosphere of Ilorin, Nigeria, *World J. Eng. Pure Appl. Sci.*, 2012, vol. 2, no. 2, pp. 56–62.
- Adebiyi, S.J., Adimula, I.A., Oladipo, O.A., Joshua, B.W., Adebesin, B.O., and Ikubanni, S.O., Ionospheric response to magnetic activity at low and mid-latitude stations, *Acta Geophys.*, 2014, vol. 62, no. 4, pp. 973–986.
<https://doi.org/10.2478/s11600-014-0205-x>
- Adekoya, B.J., Chukwuma, V.U., Bakare, N.O., and David, T.W., On the effect of geomagnetic storms and pre-storm phenomena on low and middle latitude ionospheric F2, *Astrophys. Space Sci.*, 2012, vol. 340, no. 2, pp. 217–235.
<https://doi.org/10.1007/s10509-012-1082-x>
- Adeniyi, J.O., Magnetic storm effects on the morphology of the equatorial F2-layer, *J. Atmos. Terr. Phys.*, 1986, vol. 48, no. 8, pp. 695–702.
- Adewale, A.O., Oyeyemi, E.O., Adeloye, A.B., Ngwira, C.M., and Athieno, R., Response of equatorial F region to different geomagnetic storms observed by GPS in the African Sector, *J. Geophys. Res.: Space Phys.*, 2011, vol. 116, no. A12.
<https://doi.org/10.1029/2011ja016998>
- Akala, A.O., Rabi, A.B., Somoye, E.O., Oyeyemi, E.O., and Adeloye, A.B., The response of African equatorial GPS-TEC to intense geomagnetic storms during the ascending phase of solar cycle 24, *J. Atmos. Sol. Terr. Phys.*, 2013, vol. 98, pp. 50–62.
<https://doi.org/10.1016/j.jastp.2013.02.006>
- Alagbe, G.A., Geomagnetic storm effects on F2 layer peak electron density and other profile parameters at high solar activity at an equatorial station, *J. Phys. Sci. Innovation*, 2012, vol. 4, pp. 5–12.
- Astafyeva, E., Zakharenkova, I., and Forster, M., Ionospheric response to the 2015 St. Patrick’s Day storm: A global multi-instrumental overview, *J. Geophys. Res.: Space Phys.*, 2015, vol. 120, pp. 9023–9037.
<https://doi.org/10.1002/2015JA021629>
- Bagiya, M.S., Joshi, H.P., Iyer, K.N., Aggarwal, M., Ravindran, S., and Pathan, M., TEC variations during low solar activity period (2005–2007) near the equatorial ionospheric anomaly crest region in India, *Ann. Geophys.*, 2009, pp. 1047–1057.
<https://doi.org/10.5194/angeo-27-1047-2009>
- Baishev, D.G., Moiseyev, A.V., Boroyev, R.N., Kobaykova, S.E., Mandrikova, O.V., Solovev, I.S., Khomutov, S.Yu., Polozov, Yu.A., Yoshikawa, A., and Yumoto, K., Magnetic and ionospheric observations in the Far Eastern region of Russia during the magnetic storm of 5 April 2010, *Sun Geosphere*, 2015, vol. 10, no. 2, pp. 133–140.
- Blanc, M. and Richmond, A.D., The ionospheric disturbance dynamo, *J. Geophys. Res.*, 1980, vol. 85, pp. 1669–1686.
- Buonsanto, M.J., Ionospheric storms—a review, *Space Sci. Rev.*, 1999, vol. 88, pp. 563–601.
- Buresova, D. and Laštovička, J., Pre-storm enhancements of foF2 above Europe, *Adv. Space Res.*, 2007, vol. 39, pp. 1298–1303.
- Burns, G., Solomon, S.C., Wang, W., and Killeen, T.L., The ionospheric and thermospheric response to CMEs: Challenges and successes, *J. Atmos. Sol. Terr. Phys.*, 2007, vol. 68, nos. 1–2, pp. 77–85.
- Chukwuma, V.U., On ionospheric phenomena during pre-storm and main phase of a very intense geomagnetic storm, *Acta Geophys.*, 2010, vol. 58, no. 6, pp. 1164–1192.
<https://doi.org/10.2478/s11600-010-0008-7>
- Daglis, I.A., The role of magnetosphere–ionosphere coupling in magnetic storm dynamics, in *Magnetic Storms*, Tsurutani, B.T., Gonzalez, W.D., Kamide, Y., and Arballo, J.K., Eds., Washington, D.C.: Am. Geophys. Union, 1997, vol. 98, pp. 107–116.
- Danilov, A., Ionospheric F2-region response to geomagnetic disturbances, *Adv. Space Res.*, 2013, vol. 52, pp. 343–366.
<https://doi.org/10.1016/j.asr.2013.04.019>
- Danilov, A.D. and Belik, L.D., Thermospheric composition and the positive phase of an ionospheric storm, *Adv. Space Res.*, 1992, vol. 12, no. 10, pp. 250–260.
- Danilov, A.D. and Laštovička, J., Effects of geomagnetic storms on the ionosphere and atmosphere, *Int. J. Geomagn. Aeron.*, 2001, vol. 2, pp. 209–224.
- Danilov, A.D., Belik, L.D., and Mirmovich, E.G., On a possible nature of the positive phase of ionospheric storms, *Geomagn. Aeron.*, 1985, vol. 25, pp. 768–772.
- Essex, E.A., Mendillo, M., Schodel, J.P., Klobuchar, J.A., da Rosa, A.V., Yeh, K.C., Fritz, F.H., Hibberd, R.B., Kersley, L., Koster, J.R., Matsoukas, D.A., Nakata, Y., and Roelofs, T.H., A global response of the total electron content of the ionosphere to the magnetic storm of 17 and 18 June 1972, *J. Atmos. Terr. Phys.*, 1981, vol. 43, pp. 293–306.
- Fejer, B.G., Low latitude electrodynamic plasma drifts: A review, *J. Atmos. Terr. Phys.*, 1991, vol. 53, pp. 677–693.
[https://doi.org/10.1016/0021-9169\(91\)90121-M](https://doi.org/10.1016/0021-9169(91)90121-M)
- Fejer, B.G. and Scherlies, L., Mid- and low-latitude prompt-penetration ionospheric zonal plasma drifts, *Geophys. Res. Lett.*, 1998, vol. 25, no. 16, pp. 3071–3074.
- Fejer, B.G., Larsen, M.F., and Farley, D.T., Equatorial disturbance dynamo electric fields, *Geophys. Res. Lett.*, 1983, vol. 10, pp. 537–540,
<https://doi.org/10.1029/GL010i007p00537>
- Gonzalez, W.D., Joselyn, J.A., Kamide, Y., Kroehl, H.W., Rostoker, G., Tsurutani, B.T., and Vasyliunas, V.M., What is a geomagnetic storm? *J. Geophys. Res.*, 1994, vol. 99, pp. 5771–5792.
- Gostling, J.T., McComas, D.J., Phillips, J.L., and Bame, S.J., Geomagnetic activity associated with Earth passage of interplanetary shock disturbances and coronal mass ejections, *J. Geophys. Res.*, 1991, vol. 96, pp. 7831–7839.
- Habarulema, J.B., Lee-Anne, M., Deia, B., Youngliang, Z., Gopi, S., Chigomezzyo, N., Jaroslav, C., and Ben, O., A comparative study of TEC response for the African

- equatorial and mid-latitudes during storm conditions, *J. Atmos. Sol. Terr. Phys.*, 2013, vol. 102, pp. 105–114. <https://doi.org/10.1016/j.jastp.2013.05.008>
- Joshua, B., Adeniyi, J.O., Adimula, I.A., Abbas, M., and Adebisi, S.J., The effect of magnetic storm of May 2010, on the F2-layer over the Ilorin ionosphere, *World J. Young Res.*, 2011, vol. 1, no. 5, pp. 71–78.
- Joshua, B., Adebisi, S.J., Moses, A.O., Abbas, M., Gwani, M., and Abubakar, A., Magnetic storm effects on the ionospheric F2-layer over Czech Republic, *Int. J. Emerging Technol. Adv. Eng.*, 2013, vol. 3, no. 1, pp. 1–8. <https://ijetae.com>.
- Joshua, B.W., Adeniyi, J.O., Adimula, I.A., Oladipo, O.A., Olawepo, O.A., and Adebisi, S.J., The response of the ionosphere over Ilorin to some geomagnetic storms, *Adv. Space Res.*, 2014a, vol. 54, no. 11, pp. 2224–2235. <https://doi.org/10.1016/j.asr.2014.08.027>
- Joshua, B.W., Adeniyi, J.O., Adimula, I.A., Oladipo, O.A., Olawepo, O.A., and Adebisi, S.J., Ionospheric response to the storm-time disturbance of 29 May, 2010, *Adv. Space Res.*, 2014b, vol. 53, no. 2, pp. 219–225. <https://doi.org/10.1016/j.asr.2013.11.003>
- Joshua, B.W., Adeniyi, J.O., Oladipo, O.A., Doherty, P.H., Adimula, I.A., Olawepo, O.A., and Adebisi, S.J., Simultaneous response of NmF2 and GPS-TEC to storm events at Ilorin, *Adv. Space Res.*, 2018, vol. 61, no. 12, pp. 2904–2913. <https://doi.org/10.1016/j.asr.2018.03.031>
- Kamide, Y., Baumjohann, W., Daglis, I.A., Gonzalez, W.D., Grande, M., Joselyn, J.A., McPherron, R.L., Philips, J.L., Reeves, E.G.D., Rostoker, G., Sharma, A.S., Singer, H.J., Tsurutani, B.T., and Vasyliunas, V.M., Current understanding of magnetic storms: Storm-substorm relationships, *J. Geophys. Res.*, 1998, vol. 103, no. A8, pp. 17705–17728.
- Kane, R.P., How good is the relationship of solar and interplanetary plasma parameters with geomagnetic storms?, *J. Geophys. Res.*, 1973, vol. 110, A02213. <https://doi.org/10.1029/2004JA010799>
- Kelley, M.C., Fejer, B.G., and Gonzales, C.A., An explanation for anomalous ionospheric electric fields associated with a northward turning of the interplanetary magnetic field, *Geophys. Res. Lett.*, 1979, vol. 6, no. 4, pp. 301–304. <https://doi.org/10.1029/GL006i004p00301>
- Kumar, S., Chandra, H., and Sharma, S., The equatorial anomaly crest in the Indian region, *J. Atmos. Sol. Terr. Phys.*, 2005, vol. 67, pp. 581–594.
- Laštovička, J., Effects of geomagnetic storms in the lower ionosphere, middle atmosphere and troposphere, *J. Atmos. Sol. Terr. Phys.*, 2005, vol. 66, no. 12, pp. 831–843.
- Lee Chien-Chih, Examination of the absence of noontime bite-out in equatorial total electron content, *J. Geophys. Res.*, 2012, vol. 117, A09303. <https://doi.org/10.1029/2012JA017909>
- Liu, L., Wan, W., Zhang, M.-L., Zhao, B., and Ning, B., Pre-storm enhancements in NmF2 and total electron content at low latitudes, *J. Geophys. Res.*, 2008, vol. 113, A02311. <https://doi.org/10.1029/2007JA012832>
- Low, N.C. and Roelofs, T.H., On the large scale vertical movements of the F-layer and its effects on the total electron content over low latitude during the magnetic storm of 25 May 1967, *Planet. Space Sci.*, 1973, vol. 21, no. 10, pp. 1805–1808.
- Manju, G., Kumar Pant, T., Ravindran, S., and Sridharan, R., On the response of the equatorial and low latitude ionospheric regions in the Indian sector to the large magnetic disturbance of 29 October 2003. *Ann. Geophys.*, 2009, vol. 27, pp. 2539–2544.
- Mansilla, G.A., Mid-latitude Ionospheric effect of a great geomagnetic storm, *J. Atmos. Sol. Terr. Phys.*, 2004, vol. 66, no. 12, pp. 1085–1091.
- Martyn, D.F., Ion drag with electrodynamics drift, *Proc. R. Soc. A*, 1947, vol. 189, pp. 241–260.
- Mayr, H.G. and Volland, H., Magnetic storm effects in the neutral composition, *Planet. Space Sci.*, 1972, vol. 20, pp. 379–393. [https://doi.org/10.1016/0032-0633\(72\)90036-0](https://doi.org/10.1016/0032-0633(72)90036-0)
- Mikhailov, A.V. and Perrone, L., Pre-storm NmF2 enhancements at middle latitudes: delusion or reality?, *Ann. Geophys.*, 2009, vol. 27, pp. 1321–1330.
- Olawepo, A. O., Response of ionospheric N(h) profiles over Ilorin to moderate geomagnetic storms, *Ife J. Sci.*, 2013, vol. 15, no. 3, pp. 509–521.
- Olawepo, O.A., and Adeniyi, J.O., Ionosphere's F2-layer response to 2006 geomagnetic storm at Ilorin, Nigeria, *Afr. Rev. Phys.*, 2012, vol. 7, no. 0031, pp. 277–281.
- Radicella, S.M. and Adeniyi, J.O., Equatorial ionospheric electron density below the F2 peak, *Radio Sci.*, 1999, vol. 34, no. 5, pp. 1153–1163.
- Rajaram, G. and Rastogi, R.G., Equatorial electron densities—seasonal and solar cycle changes, *J. Atmos. Terr. Phys.*, 1977, vol. 39, pp. 1175–1182. [https://doi.org/10.1016/0021-9169\(77\)90026-5](https://doi.org/10.1016/0021-9169(77)90026-5)
- Rastogi, R.G., Chandra, H., Sharma, R.P., and Girija, R., Ground-based measurements of ionospheric phenomena associated with equatorial electrojet, *Indian J. Radio Space*, 1972, vol. 1, no. 2, pp. 119–135.
- Reeves, W.D., Geomagnetism tutorial, 61.63° N:262.89° E Reeve Observatory, Anchorage, Alaska, 2010, Issue 1.0. <http://www.reeve.com/Documents/SAM/GeomagnetismTutorial.pdf>. Accessed April, 2011.
- Saranya, P.L., Venkatesh, K., Prasad, D.S.V.V.D., Rama Rao, P.V.S., and Niranjana, K., Pre-23 storm behaviour of NmF2 and TEC (GPS) over equatorial and low latitude stations in the Indian sector, *Adv. Space Res.*, 2011, vol. 48, no. 2, pp. 207–217. <https://doi.org/10.1016/j.asr.2011.03.028>
- Sastri, H., Equatorial electric field of ionospheric disturbance dynamo origin, *Ann. Geophys.*, 1988, vol. 6, pp. 635–642.
- Sastri, J.H., Effect of geomagnetic storms and sub storms on the low-latitude/equatorial ionosphere, in *ILWS Workshop 2006 on the Solar Influence on the Heliosphere and Earth's Environment*, Gopalswamy, N. and Bhat-tacharya, A., Eds., Goa, India, 2006, pp. 361–368.
- Sastri, J.H., Jyoti, N., Somayajulu, V.V., Chandra, H., and Devasia, C.V., Ionospheric storm of 30 early November 1993 in the Indian equatorial region, *J. Geophys. Res.*, 2000, vol. 105, no. A8, pp. 18443–18445. <https://doi.org/10.1029/1999JA000372>

- Scherliess, L. and Fejer, B.G., Storm time dependence of equatorial dynamo zonal electric fields, *J. Geophys. Res.*, 1997, vol. 102, pp. 24037–24046.
- Senior, C. and Blanc, M., On the control of the magnetospheric convection by the spatial distribution of ionospheric conductivities, *J. Geophys. Res.*, 1984, vol. 89, pp. 261–284.
<https://doi.org/10.1029/JA089iA01p00261>
- Sheng, C., Lu, G., Solomon, S.C., Wang, W., Doornbos, E., Hunt, L.A., and Mlynczak, M.G., Thermospheric recovery during the 5 April 2010 geomagnetic storm, *J. Geophys. Res.: Space Phys.*, 2017, vol. 122.
<https://doi.org/10.1002/2016JA023520>
- Shimeis, A., Fathy, I., Amory-Mazaudier, C., Fleury, R., Mahrous, A. M., Yumoto, K., and Groves, K., Signature of the coronal hole near the north crest equatorial anomaly over Egypt during the strong geomagnetic storm 5 April 2010, *J. Geophys. Res.*, 2012, vol. 117, A07309.
<https://doi.org/10.1029/2012JA017753>
- Shweta, M., Shivalika, S., Purohit, P.K., and Gwal, A.K., Effect of geomagnetic storms in the equatorial anomaly region observed from ground based data, *Int. J. Geomatics Geosci.*, 2010, vol. 1, no. 3, pp. 477–488.
- Skinner, N.J. and Wright, R.W., Some geomagnetic effects in the equatorial F2-region, *J. Atmos. Terr. Phys.*, 1955, vol. 6, no. 177, pp. 965–974.
- Smirnov, S., Reaction of electric and meteorological states of the near-ground atmosphere during a geomagnetic storm on 5 April 2010, *Earth Planets Space*, 2014, vol. 66, id 154.
<https://doi.org/10.1186/s40623-014-0154-2>
- Sur Dibyendu, Sarbani Ray, and Ashik Paul, *Observations of storm-time thermospheric O/N₂ ratio and TEC in the Northern Hemisphere during intense geomagnetic storms of 2015–2017*, URSI AP-RASC 2019.
- Taylor, J.R., Lester, M., and Yeoman, T.K., A superposed epoch analysis of geomagnetic storms, *Ann. Geophys.*, 1994, vol. 12, pp. 612–624.
- Titheridge, J.E. and Buonsanto, M.J., A comparison of northern and southern hemisphere TEC storm 25 behavior, *J. Atmos. Terr. Phys.*, 1988, vol. 50, pp. 763–780.
- Tsurutani, B.T. and Gonzalez, W.D., The interplanetary cause of magnetic storms: A review, in *Magnetic Storms*, Tsurutani, B.T., Gonzalez, W.D., Kamide, Y., and Arballo, J.K., Washington, D.C.: Am. Geophys. Union, 1997, vol. 98, pp. 77–89.
- Tsurutani, B.T., Sigiura, M., Iyemori, T., Goldstein, B.E., Gonzalez, W.D., Akasofu, S.I., and Smith, E.J., The nonlinear response of AE to IMF Bz driver: a spectral break at 5 hours, *Geophys. Res. Lett.*, 1990, vol. 17, no. 3, pp. 279–282.
- Tsurutani, B.T., Gonzalez, W.D., Gonzalez, A.L.C., Tang, F., Arballo, J.K., and Okada, M., Interplanetary origin of geomagnetic activity in the declining phase of the solar cycle, *J. Geophys. Res.*, 1995, vol. 100, pp. 21717–21733.
- Tsurutani, B.T., Ho, C.M., Arballo, J.K., Smith, E.J., Goldstein, B.E., Neugebauer, M., Balogh, A., Feldman, W.C., Interplanetary discontinuities and Alfvén waves at high heliographic latitudes: Ulysses, *J. Geophys. Res.*, 1996, vol. 101, no. A5, pp. 11027–11038.
<https://doi.org/10.1029/95JA03479>
- Turunen, T. and Rao, M., Examples of the influence of strong magnetic storms on the equatorial F-layer, *J. Atmos. Terr. Phys.*, 1980, vol. 42, pp. 323–330.
- Valladares, C.E., Eccles, J.V., Basu, Su., Schunk, R.W., Sheehan, R., Pradipta, R., and Ruohoniemi, J.M., The magnetic storms of 3–4 August 2010 and 5–6 August 2011: 1. Ground- and space-based observations, *J. Geophys. Res.: Space Phys.*, 2017, vol. 122, no. 3, pp. 3487–3499.
<https://doi.org/10.1002/2016JA023359>
- Webb, D.F. and Howard, R.A., The solar cycle variation of coronal mass ejections and the solar wind mass flux, *J. Geophys. Res.*, 1994, vol. 99, pp. 4201–4220.
- Woodman, R.F., Vertical drift velocities and east–west electric fields at the magnetic equator, *J. Geophys. Res.*, 1970, vol. 75, no. 31, pp. 6249–6259.
- Yizengaw, E., Dyson, P.L., Essex, E.A., and Moldwin, M.B., Ionosphere dynamics over the Southern Hemisphere during the 31 March 2001 severe magnetic storm using multi-instrument measurement data, *Ann. Geophys.*, 2005, vol. 23, pp. 707–721.
<https://doi.org/10.5194/angeo-23-707-2005>
- Zhang, Y., Paxton, I.J., Morrison, D., Wolven, B., Kil, H., Meng, C.I., Mende, S.B., and Immel, T.J., O/N₂ changes during 1–4 October 2002 storms: IMAGE SI_13 and TIMED/GUVI observations, *J. Geophys. Res.*, 2004, vol. 109, A10308.
<https://doi.org/10.1029/2004JA010441>